*Organometallics* **2001,** *20,* 5351−5359

# The Ruthenocenylmethylium Cation: Isolation and Structures of $\eta^5$-Cyclopentadienyl-$\eta^6$-fulvene-ruthenium(II) Salts

Stephen Barlow,*,[†] Andrew Cowley, Jennifer C. Green, Tim J. Brunker, and Tony Hascall

*Inorganic Chemistry Laboratory, University of Oxford, South Parks Road, Oxford, OX1 3QR, U.K.*

*Received July 25, 2001*

Salts of the ruthenocenylmethylium cation, $\mathbf{1}^+$, can be synthesized from the reaction of ruthenocenylmethanol with either Brønsted or Lewis acids. The X-ray crystal structures of the tetrakis{3,5-bis(trifluoromethyl)phenyl}borate and trifluoromethanesulfonate salts of $\mathbf{1}^+$ reveal that the methylium carbon is bound to the ruthenium with Ru−C bond lengths in the range 2.251(9)−2.40(1) Å and confirm the description of the cation structure as $\eta^5$-cyclopentadienyl-$\eta^6$-fulvene-ruthenium(II). The UV−vis spectrum of $\mathbf{1}^+$ shows a d−d transition at an energy similar to those of ruthenocene and the $\eta^5$-cyclopentadienyl-$\eta^6$-benzeneruthenium(II) cation, but with increased absorptivity. Cyclic voltammetry indicates that $\mathbf{1}^+$ is reduced at considerably less negative potential than its isomer, the $\eta^5$-cyclopentadienyl-$\eta^6$-benzene-ruthenium(II) cation. Chemical reduction with sodium amalgam in tetrahydrofuran leads to the formation of methylruthenocene, 1,2-bis(ruthenocenyl)ethane, and bis(ruthenocenylmethyl)ether. Reaction of $\mathbf{1}^+$ with triphenylphosphine affords the (ruthenocenylmethyl)triphenylphosphonium cation; the crystal structure of the dichloromethane solvate of its tetrafluoroborate salt has been determined. Density functional calculations closely reproduce the crystallographically determined geometry of $\mathbf{1}^+$ and allow rationalization of some characteristics of its structure, spectroscopy, and reactivity. The calculations suggest that the ferrocenylmethylium cation, $\mathbf{3}^+$, has a geometry similar to $\mathbf{1}^+$ with similar orbital structure, albeit with considerably more d-character to the occupied frontier orbitals.

## Introduction

The group 8 metallocenes have long been known to stabilize adjacent carbocations.[1] This stabilization arises through a direct orbital interaction between the metal and the formally cationic carbon; the interaction can be described as tending toward the structure $\eta^5$-cyclopentadienyl-$\eta^6$-fulvene-metal(II) (Figure 1a), with the positive charge formally on the metal. Back-bonding from the metal to the fulvene can be represented by contributions from a metal(IV) $\sigma$-CH$_2$ extreme structure (Figure 1b). Recently a number of studies have involved the $\eta^5$-cyclopentadienyl-$\eta^6$-fulvene-ruthenium(II) cation incorporated into various conjugated systems;[2−6] these include our own work on ruthenocene-terminated polymethine cations,[7−9] for which we were interested in comparing spectroscopic, structural, and electrochemical features of our compounds with those of the parent ruthenocenylmethylium cation, $[\mathrm{RcCH_2}]^+$, $\mathbf{1}^+$. Although there have been several studies of salts of the (nonam-

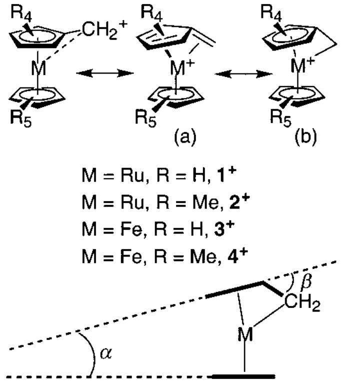

**Figure 1.** Resonance structures for metallocenyl carbocations and definition of the structural distortion angles, α and $\beta$.

---

[†] Present address: Department of Chemistry, University of Arizona, Tucson, AZ 85721.

(1) Watts, W. E. In *Comprehensive Organometallic Chemistry*; Wilkinson, G., Stone, F. G. A., Abel, E. W., Eds.; Pergamon: London, 1988; Vol. 8.

(2) Sato, M.; Kudo, A.; Kawata, Y.; Saitoh, H. *Chem. Commun.* **1996**, 25−26.

(3) Sato, M.; Kawata, Y.; Shintate, H.; Habata, Y.; Akabori, S.; Unoura, K. *Organometallics* **1997**, *16*, 1693−1701.

(4) Sato, M.; Kawata, Y.; Kudo, A.; Iwai, A.; Saitoh, H.; Ochiai, S. *J. Chem. Soc., Dalton Trans.* **1998**, 2215−2224.

(5) Sato, M.; Iwai, A.; Watanabe, M. *Organometallics* **1999**, *18*, 3208−3219.

(6) Watanabe, M.; Sato, M.; Takayama, T. *Organometallics* **1999**, *18*, 5201−5203.

(7) Barlow, S.; Henling, L. M.; Day, M. W.; Marder, S. R. *Chem. Commun.* **1999**, 1567−1568.

(8) Barlow, S.; Day, M. W.; Marder, S. R. *Acta Crystallogr.* **2000**, *C56*, 303−304.

(9) Barlow, S.; Henling, L. M.; Day, M. W.; Schaefer, W. P.; Green, J. C.; Hascall, T.; Marder, S. R. Manuscript in preparation.

10.1021/om010667+ CCC: $20.00

**Scheme 1**

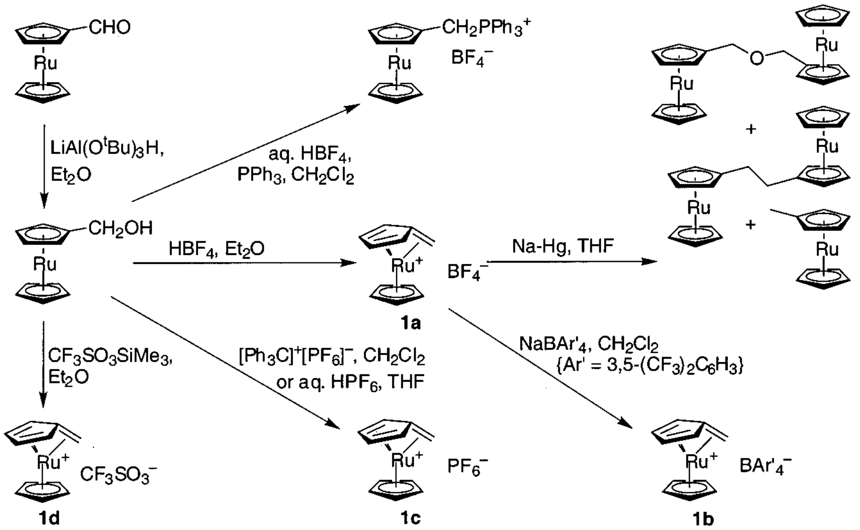

ethylruthenocenyl)methylium cation, $\mathbf{2}^+$,[10−13] there has been little work published on its unsubstituted analogue. Although $\mathbf{1}^+$ has been recognized as an intermediate, for example in the solvolysis of $RcCH_2OAc$,[14] and its p$K_{R^+}$ value has been determined,[15] we are not aware of any reports of the isolation of its salts. In this paper we report on the synthesis, characterization, structures, and reactivity of $\mathbf{1}^+$ salts.

## Results and Discussion

**Synthesis.** $RcCH_2OH$ (Rc = ruthenocenyl) has previously been synthesized from $[RcCH_2NMe_3]^+[I]^-$ [16] and by $NaBH_4$ reduction of RcCHO.[17] We obtained the alcohol from RcCHO[18] using $LiAl(O^tBu)_3H$, by analogy with the method described for $RuCp^*(\eta^5\text{-}C_5Me_4CH_2OH)$[10] (Scheme 1). Treatment of an ether solution of the alcohol with ethereal $HBF_4$ afforded a pale cream precipitate, identified by NMR spectroscopy and analytical data as $[RcCH_2]^+[BF_4]^-$, **1a**. $[RcCH_2]^+[BAr'_4]^-$ {Ar′ = 3,5-bis(trifluoromethyl)phenyl}, **1b**, was obtained from **1a** by using the method described by Manríquez and co-workers for the synthesis of $[FeCp_2]^+[BAr'_4]^-$.[19] $[RcCH_2]^+[PF_6]^-$, **1c**, can be synthesized from the alcohol by treatment with either aqueous $HPF_6$ in THF or $[Ph_3C]^+[PF_6]^-$ in dichloromethane, while $[RcCH_2]^+[CF_3SO_3]^-$, **1d**, was precipitated by the addition of $CF_3SO_3SiMe_3$ to an ether solution of the alcohol. The analogous ferrocenylmethylium cation, $\mathbf{3}^+$, is complexed by ether molecules when its salts are precipitated from various ethers;[20] in contrast, the salts of $\mathbf{1}^+$ show no evidence (elemental analysis, NMR, crystallography) for this type of behavior.

Since trityl salts have been used to abstract hydride from $Mc(CH{=}CH)_nCH_2(CH{=}CH)_nMc$ {Mc = ferrocenyl, $n$ = 1, 2, 3;[21] Mc = Rc, $n$ = 1[22]}, we also attempted to synthesize the (1′-methylruthenocenyl)methylium cation from the analogous reaction with 1,1′-dimethylruthenocene. A mixture of products was formed, and the target cation could not be isolated.

Salts of $\mathbf{1}^+$ appear to be indefinitely stable under nitrogen, both in the solid state and in dichloromethane solution, in contrast to ferrocene analogues, which rapidly dimerize to bis(ferroceniumyl)ethanes.[23−26] When exposed to air, solid cream-colored $\mathbf{1}^+$ salts decompose to black material on a time scale of weeks; solutions decompose more rapidly. Solutions of $\mathbf{1}^+$ in acetonitrile or nitromethane slowly turn yellowish on standing, even in the absence of air; $^1H$ NMR spectroscopy reveals a complex mixture of products.

Triphenylphosphine reacts with $\mathbf{1}^+$ at the exo position to afford $[RcCH_2PPh_3]^+$; this is consistent with the large LUMO coefficient on the exo carbon (vide infra, Figure 6). Accordingly, $RcCH_2OH$ can be converted to $[RcCH_2PPh_3]^+[BF_4]^-$ using a method analogous to that described for $FcCH_2OH$[27,28] and RcCHROH {R = Me, Ph}.[29] The $[RcCH_2PPh_3]^+$ cation has previously been obtained from $[RcCH_2NMe_3]^+$.[30]

---

(10) Kreindlin, A. Z.; Petrovskii, P. V.; Rybinskaya, M. I.; Yanovskii, A. I.; Struchkov, Y. T. *J. Organomet. Chem.* **1987**, *319*, 229−237.

(11) Yanovsky, A. I.; Struchkov, Y. T.; Kreindlin, A. Z.; Rybinskaya, M. I. *J. Organomet. Chem.* **1989**, *369*, 125−130.

(12) Kirchner, K.; Dasgupta, S.; Schmid, R. *J. Chem. Res. S* **1993**, 340−1.

(13) Kamyshova, A. A.; Kreindlin, A. Z.; Rybinskaya, M. I.; Petrovskii, P. V. *Russ. Chem. Bull.* **1999**, *48*, 581−585.

(14) Hill, E. A.; Richards, J. H. *J. Am. Chem. Soc.* **1961**, *83*, 3840−3846.

(15) Tang, J.; Top, S.; Vessières, A.; Sellier, N.; Vaissermann, J.; Jaouen, G. *Appl. Organomet. Chem.* **1997**, *11*, 771−781.

(16) Hofer, O.; Schlögl, K. *J. Organomet. Chem.* **1968**, *13*, 443−456.

(17) Schneider, M.; Wenzel, M. *J. Labeled Compd. Radiopharm.* **1980**, *17*, 1−20.

(18) Sanders, R.; Mueller-Westerhoff, U. T. *J. Organomet. Chem.* **1996**, *512*, 219−224.

(19) Chávez, I.; Alvarez-Carena, A.; Molins, E.; Roig, A.; Maniukiewicz, W.; Aranacibia, A.; Aranacibia, V.; Brand, H.; Manríquez, J. M. *J. Organomet. Chem.* **2000**, *601*, 126−132.

(20) Ceccon, A.; Giacometti, G.; Venzo, A.; Paolucci, D.; Benozzi, D. *J. Organomet. Chem.* **1980**, *185*, 231−239.

(21) Tolbert, L. M.; Zhao, X.; Ding, Y.; Bottomley, L. A. *J. Am. Chem. Soc.* **1995**, *117*, 12891−12892.

(22) Barlow, S. Unpublished results.

(23) Rinehart, K. L.; Michejda, C. J.; Kittle, P. A. *J. Am. Chem. Soc.* **1959**, *81*, 3162−3163.

(24) Fedin, E. I.; Blumenfeld, A. L.; Petrovskii, P. V.; Kreindlin, A. Z.; Fadeeva, S. S.; Rybinskaya, M. I. *J. Organomet. Chem.* **1985**, *292*, 257−268.

(25) Zou, C.; Wrighton, M. S. *J. Am. Chem. Soc.* **1990**, *112*, 7578−7584.

(26) Bildstein, B.; Hradsky, A.; Kopacka, H.; Malleier, R.; Ongania, K.-H. *J. Organomet. Chem.* **1997**, *540*, 127−145.

(27) Boev, V. I.; Dombrovskii, A. V. *Zh. Obshch. Khim.* **1984**, *54*, 1192−1197.

(28) Boev, V. I.; Dombrovskii, A. V. *J. Gen. Chem. USSR* **1984**, *54*, 1067−1071.

(29) Boev, V. I. *Zh. Org. Khim.* **1992**, *28*, 770−778.

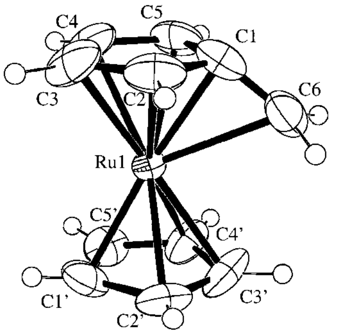

**Figure 2.** View of the **1**$^+$ cation of in the crystal structure of **1b** (non-hydrogen atoms are shown with 50% thermal ellipsoids, hydrogen atoms as spheres of arbitrary radius). The cation lies on a crystallographic 2-fold rotation axis and so is required to be disordered; the cyclopentadienyl rings are related by the 2-fold axis, with C6 modeled at half-occupancy. The symmetry-generated C6′ is omitted from this view.

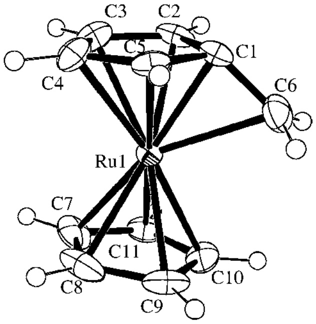

**Figure 3.** View of the nondisordered **1**$^+$ cation in the crystal structure of **1d** (non-hydrogen atoms are shown with 50% thermal ellipsoids, hydrogen atoms as spheres of arbitrary radius).

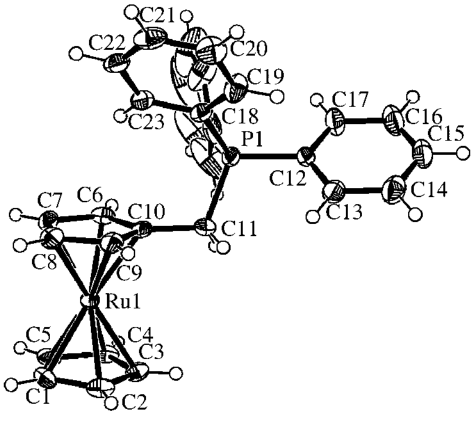

**Figure 4.** View of the $[RcCH_2PPh_3]^+$ cation in the crystal structure of $[RcCH_2PPh_3]^+[BF_4]^- \cdot 0.5CH_2Cl_2$ (non-hydrogen atoms are shown with 50% thermal ellipsoids, hydrogen atoms as spheres of arbitrary radius). The atom labels are omitted from one of the phenyl groups for clarity.

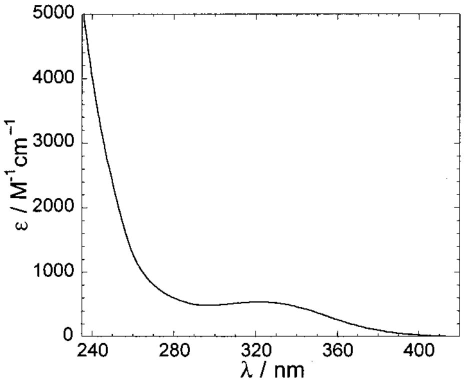

**Figure 5.** UV-vis spectrum of **1a** in dichloromethane.

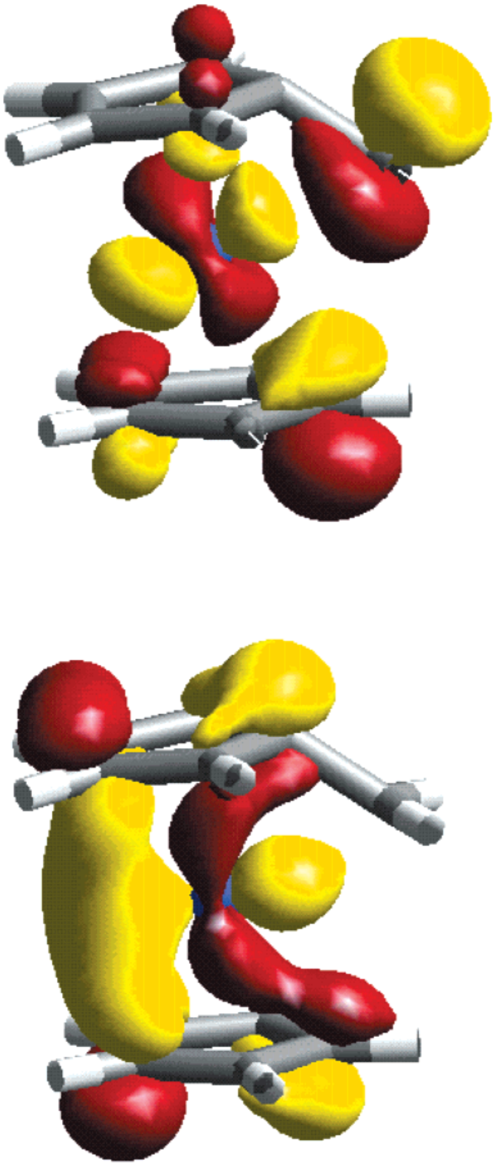

**Figure 6.** LUMO (top) and HOMO-3 (bottom) of **1**$^+$ according to density functional calculations. These orbitals are broadly similar to the LUMO and HOMO-2 respectively of **3**$^+$.

**Crystal Structures.** The crystal structures of **1b** and **1d** were determined by single-crystal X-ray diffraction. In both cases the structures are complicated by disorder. The cation in **1b** (Figure 2) is disordered due to its location on a crystallographic 2-fold axis, while the asymmetric unit of **1d** contains four distinct cations, two of which are disordered over inversion centers, one of which shows thermal parameters indicative of unresolved disorder, and one of which is fully ordered (Figure 3, Table 1). Nevertheless, in all these cations it is clear that the $CH_2$ group is coordinated to the metal. The

---

(30) Bunting, H. E.; Green, M. L. H.; Marder, S. R.; Thompson, M. E.; Bloor, D.; Kolinsky, P. V.; Jones, R. J. *Polyhedron* **1992**, *11*, 1489–1499.

**Table 1. Comparison of Crystallographically Determined Parameters for $1^+$ with DF-Calculated Parameters for $1^+$ and $3^+$**

| bond lengths, angles[a]/Å, deg | crystal structure[b] | calculated using LDA-DFT | |
|---|---|---|---|
| | $1^+$ | $1^+$ | $3^+$ |
| M−C1 | 2.080(4) | 2.075 | 1.924 |
| M−C2 | 2.177(4) | 2.185 | 2.026 |
| M−C3 | 2.245(4) | 2.254 | 2.081 |
| M−C4 | 2.235(4) | 2.254 | 2.079 |
| M−C5 | 2.175(4) | 2.183 | 2.024 |
| M−C6 | 2.272(4)[c] | 2.263 | 2.161 |
| M−$C_{C5H5}$, range | 2.187(4)−2.215(4) | 2.185−2.212 | 2.024−2.058 |
| M−$C_{C5H5}$, av | 2.194(13) | 2.199(13) | 2.040(16) |
| C1−C2 | 1.458(6) | 1.455 | 1.450 |
| C1−C5 | 1.459(6) | 1.452 | 1.450 |
| C1−C6 | 1.405(6) | 1.403 | 1.396 |
| C2−C3 | 1.413(7) | 1.408 | 1.405 |
| C3−C4 | 1.429(6) | 1.430 | 1.428 |
| C4−C5 | 1.412(6) | 1.406 | 1.405 |
| $C_{C5H5}$−$C_{C5H5}$, range | 1.414(8)−1.425(7) | 1.420−1.427 | 1.417−1.428 |
| $C_{C5H5}$−$C_{C5H5}$, av | 1.418(6) | 1.424(3) | 1.421(4) |
| α | 7.1 | 5.3 | 10.5 |
| $\beta$ | 42.6 | 41.2 | 44.0 |

[a] Atom labeling is that shown in Figure 3; angles α (ring tilt) and $\beta$ (angle between $C_{Cp}$−$C_{exo}$ and the attached ring) are defined in Figure 1. [b] Parameters for the ordered cation in the crystal structure of **1d**. [c] Range for all the cations in the structures of **1b** and **1d** is 2.251(9)−2.40(1) Å.

R−$C_{CH2}$ bond lengths in **1b** and **1d**, which should be little affected by the disorder, fall in the range 2.251(9)−2.40(1) Å; the value for the nondisordered cation of **1d** is 2.272(4) Å. The corresponding value for $2^+$ in the dichloromethane solvate of its tetraphenylborate salt is 2.270(3) Å,[11,31] and values in the range 2.281(9)−2.571(4) Å have been reported for other more complex ruthenocenyl carbocations.[4,5,7−9,32,33] The average Ru−$C_{Cp}$ and Ru−$C_{fulvene}$ bond lengths in the nondisordered cation of **1d** are not significantly different from each other, or from the corresponding distances in $2^+$, in $[(\eta^6\text{-arene})RuCp]^+$ derivatives,[34−36] or in ruthenocene itself.[37] The C−C bond lengths within the $C_5H_4CH_2$ ligand of the nondisordered cation of **1d** show significant alternation similar to that seen for $2^+$[11] and for some susbtituted ($\eta^6$-fulvene)Cr(CO)$_3$ derivatives,[38] consistent with the description of the $C_5H_4CH_2$ ligand as coordinated fulvene. In each $1^+$ cation it is also evident that the fulvene ligand is nonplanar; in the nondisordered cation of **1d** the angle, $\beta$ (Figure 1), between the $C_{Cp}$−$C_{CH2}$ bond and the attached five-membered ring is 42.6°, while in the other cations of **1d** and that of **1b** the apparent value of this angle is somewhat affected by disorder. The corresponding angle in the structure of $2^+[BPh_4]^-\cdot CH_2Cl_2$ is 40.3°,[11] and $\beta$ falls in the range 29.9−40.4° for other systems.[4,5,7−9,32,33] The coordination of $CH_2$ to the Ru also leads to the two five-membered rings being nonparallel. In the nondisordered cation of **1d** this ring tilt, α (Figure 1), is 7.1°. Disorder affects the apparent value of α in the other cations; in the two cations of **1d** which lie on inversion centers this effect is especially severe, the crystallographic symmetry causing the rings to appear parallel (α = 0). The ring tilt for $2^+[BPh_4]^-\cdot CH_2Cl_2$ is 9.0°.[11] The two five-membered rings of the $1^+$ cations vary from almost perfectly eclipsed conformation (in **1b**) to perfectly staggered (the disordered cations of **1d**), with intermediate cases (the ordered cation of **1d**). In summary, crystallographic data show $1^+$ and $2^+$ have very similar geometry.

The crystal structure of $[RcCH_2PPh_3]^+[BF_4]^-\cdot xCH_2Cl_2$ $\{x = \text{ca. } 0.5\}$ has also been determined and confirms the molecular structure, as shown in Figure 4. In contrast to the $CH_2$ group of **1b** and **1d**, that of the $[RcCH_2PPh_3]^+$ cation does not interact with the ruthenium center; the $C_{Cp}$−$C_{CH2}$ bond is actually bent very slightly away from the metal leading to a Ru−$C_{CH2}$ distance of 3.290(6) Å. The ring tilt is only 1.5°, and the Ru−$C_{Cp}$ distances range from 2.158(5) to 2.190(5) Å (average 2.173(10) Å), similar to those for other "normal" ruthenocenes. Thus, $[RcCH_2PPh_3]^+$ is a "normal" phosphonium salt. The two cyclopentadienyl rings are approximately eclipsed.

**Spectroscopy.** In the $^1H$ NMR spectrum, the $CH_2$ resonance of **1a** is observed at 5.07 ppm in $CD_2Cl_2$ and at 5.25 ppm in acetone-$d_6$, and that of **1c** is at 5.02 ppm in $CD_2Cl_2$; for $2^+$ a corresponding value of 4.75 ppm has been reported, both for the tetrafluoroborate in acetone-$d_6$[10] and for the hexafluorophospate in $CD_2Cl_2$.[39] The $CH_2$ $^{13}C$ resonance of **1a** is seen at 72.7 ppm in $CD_2Cl_2$; values of 77.8[10] and 74.7[39] ppm have been reported for the corresponding shifts of the hexafluorophosphate of $2^+$ in $CH_2Cl_2$. The decrease in $^1H$ shift and increase in $^{13}C$ shift brought about by methylation perhaps reflect the presence of opposing effects; presumably the inductive effect of the methyl groups and the interaction with the metal are both important factors. The $CH_2$ resonances for the ruthenium species, $1^+$ and $2^+$, are at consistently lower frequency than those of their iron analogues; values for the $CH_2$ $^1H$ resonance of the ferrocenylmethylium cation, $3^+$, have been reported in the range 5.75−6.00 ppm for a variety of solvents and counterions,[20,40−42] while for the (nonamethylferrocenyl)methylium ion, $4^+$, the $CH_2$ $^1H$ and $^{13}C$ resonances are in the ranges 4.98−5.29 and 90.7−91.2 ppm, respectively.[24,43] The cyclopentadienyl $^1H$ and $^{13}C$ NMR resonances of $1^+$ are at considerably higher frequency than those of simple ruthenocenes. The $C_5H_5$ $^1H$ chemical shifts allow one to compare the ligand properties of fulvene with those of its isomer, benzene; in acetone-$d_6$ these resonances are at 5.70 and 5.45 ppm for **1a** and $\eta^5$-cyclopentadienyl-$\eta^6$-benzene-ruthenium(II) hexafluorophosphate,[44] respectively (ruthenocene is at 4.60 ppm

---

(31) The structure of the hexafluorophosphate of $2^+$ has also been reported (see ref 10), but the parameters reported are seriously affected by disorder.

(32) Watanabe, M.; Moyoyama, I.; Takayama, T. *J. Organomet. Chem* **1996**, *524*, 9−18.

(33) Watanabe, M.; Motoyama, I.; Takayama, T. *Bull. Chem. Soc. Jpn*. **1996**, *69*, 2877−2884.

(34) Huckett, S. C.; Miller, L. L.; Jacobson, R. A.; Angelici, R. J. *Organometallics* **1988**, *7*, 686−691.

(35) Fagan, P. J.; Ward, M. D.; Calabrese, J. C. *J. Am. Chem. Soc.* **1989**, *111*, 1698−1719.

(36) Nolan, S. P.; Martin, K. L.; Stevens, E. D. *Organometallics* **1992**, *11*, 3947−3953.

(37) Seiler, P.; Dunitz, J. D. *Acta Crystallogr.* **1980**, *B36*, 2946−2950.

(38) Lubke, B.; Edelmann, F.; Behrens, U. *Chem. Ber.* **1983**, *116*, 11−26.

(39) Kreindlin, A. Z.; Fedin, E. I.; Petrovskii, P. V.; Rybinskaya, M. I.; Minyaev, R. M.; Hoffmann, R. *Organometallics* **1991**, *10*, 1206−1209.

(40) Cais, M.; Dannenberg, J. J.; Eisenstadt, A.; Levenburg, M. I.; Richards, J. H. *Tetrahedron Lett.* **1966**, 1695−1701.

(41) Histame, M.; Yamakawa, K. *Tetrahedron* **1971**, *27*, 2101−2110.

(42) Cerichelli, G.; Floris, B.; Ortaggi, G. *J. Organomet. Chem.* **1974**, *78*, 241−252.

(43) Kreindlin, A. Z.; Dolgushin, F. M.; Yanovsky, A. I.; Kerzina, Z. A.; Petrovskii, P. V.; Rybinskaya, M. I. *J. Organomet. Chem.* **2000**, *616*, 106−111.

in this solvent), suggesting fulvene is a more “electron-poor” ligand than benzene when coordinated to [Ru($\eta^5$-$C_5H_5$)]$^+$.[45]

The UV−vis spectrum of **1a** is shown in Figure 5. The feature at ca. 320 nm is similar in energy to the spin-allowed d−d transitions of both ruthenocene[46] and the $\eta^5$-cyclopentadienyl-$\eta^6$-benzene-ruthenium(II) cation;[47] the considerably increased absorptivity in the present compound presumably indicates relaxation of the parity selection rule due to the lower symmetry of the ligand field. Calculations (vide infra) confirm that the HOMO and particularly the LUMO of **1**$^+$ have far-from-ideal inversion symmetry. The higher energy part of the spectrum resembles the $\eta^5$-cyclopentadienyl-$\eta^6$-benzene-ruthenium(II) spectrum more closely than that of ruthenocene; the onset of intense, presumably charge-transfer, absorption appears at a similar energy in **1a** and the benzene complex.

**Redox Chemistry.** Cyclic voltammetry of **1a** in acetonitrile reveals an irreversible reduction at −1450 mV vs ferrocenium/ferrocene, while $\eta^5$-cyclopentadienyl-$\eta^6$-benzene-ruthenium(II) hexafluorophosphate is irreversibly reduced at −2420 mV in the same solvent.[48,49] The greater ease of reduction of **1**$^+$ is consistent with the NMR evidence that fulvene acts as a more “electron-poor” ligand than benzene (vide supra). In dichloromethane, the reduction peak is observed at −1235 mV; the electron transfer appears to be a little more reversible in this solvent, with a weak reverse wave observed, and $E_{1/2}$ may be estimated as ca. −1110 mV. This may be compared to values of $E_{1/2}$ of −730, −830, −760, and −640 mV for [Rc(CH)$_3$Fc]$^+$, [Rc(CH)$_3$Fc″]$^+$ {Fc″ = 2,3,4,5,1′,2′,3′,4′-octamethylferrocen-1-yl}, [Rc(CH)$_3$Rc]$^+$, and [Rc(CH)$_5$Rc]$^+$, respectively, in the same solvent.[9,22] The greater ease of reduction for these ter- and pentamethine species relative to **1**$^+$ may be attributed to the differences between the LUMOs (Figure 6 for **1**$^+$; Figure 9 of ref 50 for [Rc(CH)$_3$Rc]$^+$). Chemical reduction with sodium amalgam in THF afforded a mixture of products, which were separated by column chromatography to give low yields of the new compound RcCH$_2$CH$_2$Rc and of RcCH$_2$OCH$_2$Rc (which has previously been observed as a side product from the chromatography of RcCH$_2$OH on alumina[16,17] and presumably arises from reaction of **1**$^\bullet$ with the solvent, or of **1**$^+$ with any traces of NaOH present), as well as a trace of the known compound RcMe.[16,51]

These results may be compared to those for $\eta^5$-cyclopentadienyl-$\eta^6$-benzene-ruthenium(II) cation; reduction with sodium amalgam under conditions similar to ours has been reported to give varying ratios of $\eta^5$-cyclopentadienyl-$\eta^5$-cyclohexadienylruthenium (presumably resulting from the 19-electron Ru(I) species abstracting H$^\bullet$ from a solvent or other molecule, paralleling our observation of RcMe) and ruthenocene (presumably formed by ligand exchange) as the main isolable products.[48,52] Products arising from dimerization of the reduced species through the arene, paralleling our observation of RcCH$_2$CH$_2$Rc, have been observed for other $\eta^5$-cyclopentadienyl-$\eta^6$-areneruthenium(II) derivatives; in these cases the dimerization leads to a $\mu$-$\eta$:$^5\eta^5$-1,1′-dihydrobiphenyl (or a similar derivative) ligand.[48] The dimerization of **1**$^\bullet$ is also reminiscent of the reaction of FcCHROH {where R can be various alkyl groups} with Zn/HCl to give FcCHRCHRFc; it is thought that the ferrocenyl carbocation is formed initially and then reduced to [FcCHR]$^\bullet$.[53] The reactivity of **1**$^\bullet$ and [FcCHR]$^\bullet$ through the exo-carbon presumably reflects the high LUMO coefficient of **1**$^+$ and **3**$^+$, and thus high SOMO coefficient for **1**$^\bullet$ and **3**$^\bullet$, on this carbon (vide infra, Figure 6).

**Density Functional Calculations.** To rationalize features of the structure, spectroscopy, and reactivity of **1**$^+$, and to gain insight into the structure of its iron analogue, **3**$^+$, for which crystallographic data are unavailable (due to its instability with respect to dimerization to 1,2-bis(ferroceniumyl)ethane), we performed density functional (DF) calculations. Minimization of the geometry of **1**$^+$ using the local density approximation (LDA) gave structural parameters in excellent agreement with the corresponding values for the ordered cation in the structure of **1d** (Table 1). The corresponding LDA-DF-derived parameters for **3**$^+$ are also given in Table 1 and suggest geometry quite similar to that for **1**$^+$. Other DF methods including gradient corrections (such as the BLYP method, see Experimental Section) gave somewhat longer M−C bond distances and lower values for $\beta$, but the general pattern of bond lengths and angles was the same.

A previous MNDO/AM1 study gave a geometry similar to our LDA-DF structure for **1**$^+$ with $\beta = 41.5°$, but gave a very different $\beta$ of 5.0° for **3**$^+$,[54] while an extended-Hückel study of **3**$^+$ gave $\beta = 40°$, although the authors believed this was somewhat overestimated.[55] Since the submission of our paper, BLYP-DF calculations have been reported for **2**$^+$ (M−C$_{CH2}$, 2.410 Å; $\beta$, 32.4°) and **4**$^+$ (2.324 Å, 34.0°)[56] and give geometries similar to our calculations using the same method for **1**$^+$ (2.368 Å, 35.8°) and **3**$^+$ (2.278 Å, 37.8°), respectively. The disparities between the crystallographic[11,43] and BLYP-DF[56] values of M−C$_{CH2}$ and $\beta$ for **2**$^+$ and **4**$^+$ have been attributed to crystal-packing effects. Further evidence that these parameters are particularly sensi-

---

[44] Nesmeyanov, A. N.; Vol'kenau, N. A.; Bolesova, I. N.; Shul'pina, L. S. *J. Organomet. Chem.* **1979**, *182*, C36−C38.

[45] For [Ru($\eta^6$-C$_5$Me$_4$CH$_2$)Cp]$^+$ NMR data in acetonitrile-$d_3$ have been reported in ref 3; the CH$_2$ $^1$H and $^{13}$C resonances were observed at 5.05 and 69.4 ppm, respectively, and the Cp $^1$H and $^{13}$C resonances were seen at 5.19 and 85.9 ppm, respectively. The different solvent means these data are not directly comparable with the data discussed here for **1**$^+$, **2**$^+$, and [Ru($\eta^6$-benzene)Cp]$^+$.

[46] Sohn, Y. S.; Hendrickson, D. N.; Gray, H. B. *J. Am. Chem. Soc.* **1971**, *93*, 3603−3612.

[47] Gill, T. P.; Mann, K. R. *Organometallics* **1982**, *1*, 485−488.

[48] Gusev, O. V.; Ievlev, M. A.; Peterleitner, M. G.; Peregudova, S. M.; Denisovich, L. I.; Petrovskii, P. V.; Ustynyuk, N. A. *J. Organomet. Chem.* **1997**, *534*, 57−66.

[49] Using a correction of $E_{1/2}$(ferrocenium/ferrocene) = +400 mV vs SCE (Connelly, N. G.; Geiger, W. E. *Chem. Rev.* **1996**, *96*, 877−910).

[50] Barlow, S.; Marder, S. R. *Chem. Commun.* **2000**, 1555−1562, and references therein.

[51] Albers, M. O.; Liles, D. C.; Robinson, D. J.; Shaver, A.; Singleton, E.; Wiege, M. B.; Boeyens, J. C. A.; Levendis, D. C. *Organometallics* **1986**, *5*, 2321−2327.

[52] Vol'kenau, N. A.; Bolesova, I. N.; Shul'pina, L. S.; Kitaigorodskii, A. N. *J. Organomet. Chem.* **1984**, 313−321.

[53] Cais, M.; Eisenstadt, A. *J. Org. Chem.* **1965**, *30*, 1148−1154.

[54] Gal'pern, E. G.; Gambaryan, N. P.; Kreindlin, A. Z.; Rybinskaya, M. I.; Stankevich, I. V.; Chistyakov, A. L. *Metalloorg. Khim.* **1992**, *5*, 831−838.

[55] Gleiter, R.; Seeger, R. *Helv. Chim. Acta* **1971**, *54*, 1217−1220.

[56] Rybinskaya, M. I.; Nekrasov, Y. S.; Borisov, Y. A.; Belokon', A. I.; Kreindlin, A. Z.; Kamyshova, A. A.; Kruglova, N. V. *J. Organomet. Chem.* **2001**, *631*, 9−15.

**Table 2. Energies and d-Orbital Content of Some Frontier Orbitals of $1^+$ and $3^+$ According to DF Calculations**[a]

| | $\mathbf{1}^+$ | | $\mathbf{3}^+$ | |
|---|---|---|---|---|
| | energy/eV | % d | energy/eV | % d |
| LUMO | −6.45 | 40 | −7.02 | 49 |
| HOMO | −9.72 | 76 | −9.41 | 82 |
| HOMO-1 | −9.75 | 79 | −9.53 | 82 |
| HOMO-2 | | | −10.63 | 66 |
| HOMO-3 | −10.95 | 47 | | |

[a] The HOMO-3 of $\mathbf{1}^+$ corresponds to the HOMO-2 of $\mathbf{3}^+$ (see text).

tive to crystal packing comes from the range of M−$C_{CH2}$ values (2.251(9) to 2.40(1) Å) found for the five crystallographically distinct $\mathbf{1}^+$ cations in the crystal structures of **1b** and **1d** and from the variation in $\beta$ and Ru−$C_{CH2}$ observed between the tetrafluoroborate[32] and hexafluorophosphate[33] of a mixed iron−ruthenium [1.1]metallocenophane carbocation, and between $[Rc(CH)_3Rc]^+[PF_6]^-$[7] and $[Rc(CH)_3Rc]^+[BAr'_4]^-$.[9] In addition, while BLYP-DF calculations predict a shorter M−$C_{CH2}$ distance for $\mathbf{4}^+$ than $\mathbf{2}^+$, and while we find shorter M−$C_{CH2}$ for $\mathbf{3}^+$ than $\mathbf{1}^+$ using a variety of DF methods, the structure of $\mathbf{4}^+[BAr'_4]^-$ (the only crystallographically characterized ferrocenyl carbocation free of additional stabilizing substituents) exhibits an Fe−$C_{CH2}$ bond length of 2.57(1) Å,[43] *longer* than the corresponding distance in that of $\mathbf{2}^+[BPh_4]^-\cdot CH_2Cl_2$ (2.270(3) Å),[11] and a $\beta$ of 23.6°.[43] Nevertheless, BLYP-DF calculations, both in our present study of $\mathbf{1}^+$ and $\mathbf{3}^+$ and in the previous study of $\mathbf{2}^+$ and $\mathbf{4}^+$,[56] also consistently overestimate other M−C and C−C bond lengths relative to crystallographic data. Thus, it seems that the LDA-DF structure (i.e., that summarized in Table 1) is likely to be a better approximation to the gas-phase structure of $\mathbf{3}^+$, although the degree of bending of the $CH_2$ toward the iron atom may be very different in condensed phases.

The DF-derived orbital schemes for $\mathbf{1}^+$ and $\mathbf{3}^+$ are broadly similar. The frontier orbitals of both species have considerable d-character (Table 2), although the orbitals have far from ideal inversion symmetry, consistent with the high absorptivity of the "d−d transition" for $\mathbf{1}^+$ (vide supra). There is less d-contribution to both HOMO and LUMO for the ruthenium species, reflecting stronger forward-bonding and back-bonding. The LUMOs (shown in Figure 6 for $\mathbf{1}^+$; the corresponding orbital for $\mathbf{3}^+$ is broadly similar in appearance) are reminiscent of those of axially symmetric $d^6$ sandwich compounds, such as ferrocene and bis(benzene)chromium, where the LUMO is a d-ligand antibonding orbital having $\pi_g$ symmetry (for ideal axial $D_{\infty h}$-symmetry, corresponding to $e_{1g}$ in $D_{5d}$) with respect to the M-ligand axis. However, a notable feature of the LUMO of $\mathbf{1}^+$ and $\mathbf{3}^+$ is the large coeffecient on the $CH_2$ carbon, consistent with the sites of reaction observed for $\mathbf{1}^+$ and $\mathbf{1}^\bullet$ (vide supra). The HOMO and HOMO-1 of $\mathbf{1}^+$ and $\mathbf{3}^+$ are largely d in character, as are those of axially symmetric $d^6$ sandwich compounds. The remaining filled d-based orbital interacts strongly with the LUMO of the fulvene fragment (Figure 6); it consequently has much reduced d-character relative to the HOMO and HOMO-1 and is considerably lower in energy. For $\mathbf{3}^+$ this orbital is the HOMO-2, but for $\mathbf{1}^+$ the d-fulvene interaction is sufficiently strong to push this orbital below one of the ligand-based orbitals (analogous to the $\pi_u$ level in axially symmetric sandwich species, i.e., to $e_{1u}$ in $D_{5d}$), so it is the HOMO-3. The occupancies of the fulvene fragment LUMO resulting from this interaction are found to be 0.60 and 0.56 for $\mathbf{1}^+$ and $\mathbf{3}^+$, repectively, consistent with the longer $C_{Cp}$−$C_{exo}$ bond calculated in the ruthenium compound and corresponding to more contribution from the resonance structure (b) of Figure 1 in $\mathbf{1}^+$ than in $\mathbf{3}^+$.

The HOMO−LUMO gap for $\mathbf{1}^+$ (3.27 eV) is of the same order of magnitude as the observed lowest energy transition in the UV−vis (vide supra). Moreover, the gap for $\mathbf{3}^+$ (2.39 eV) is considerably smaller, consistent with the lower energy visible absorption reported for ferrocenyl carbocations (they are reported to be orange or red) and with the smaller singlet−triplet separations suggested to be responsible for their dimerization to bis(ferroceniumyl)ethanes.[57]

## Summary

Salts of the simplest ruthenocenyl carbocation, $[RcCH_2]^+$, have been isolated for the first time; their structures, spectroscopy, electrochemistry, and reactivity have been investigated and compared with substituted derivatives and with the isoelectronic $\eta^5$-cyclopentadienyl-$\eta^6$-arene-ruthenium(II) cations. Crystallographic data confirm that the formally cationic carbon is coordinated to the ruthenium and that the structure is best described as $\eta^5$-cyclopentadienyl-$\eta^6$-fulvene-ruthenium(II). Density functional theory gave an optimized geometry for $[RcCH_2]^+$ in good agreement with the crystallographic data and suggested a similar structure for the $[FcCH_2]^+$ cation.

## Experimental Details

Electrochemistry was performed using deoxygenated solutions, ca. $10^{-4}$ M in sample and 0.1 M in $[^nBu_4N]^+[PF_6]^-$, in freshly distilled dried solvents, Pt wire auxiliary and pseudoreference electrodes, and a glassy carbon working electrode. Ferrocene was used as an internal reference. Solvents were dried by distillation from sodium−benzophenone (diethyl ether), sodium−potassium alloy (pentane), potassium (THF), or calcium hydride (dichloromethane, acetonitrile).

**RcCH₂OH.** A solution of *tert*-butyl alcohol (distilled from $CaH_2$; 4.25 mL, 45 mmol) in diethyl ether (15 mL) was added dropwise to a suspension of $LiAlH_4$ (purified by dissolution in diethyl ether and filtration, 600 mg, 15 mmol) in diethyl ether (15 mL). When the addition was complete, a solution of RcCHO[18] (544 mg, 2.10 mmol) in diethyl ether (50 mL) was added dropwise. After stirring for 2 h at room temperature, water (50 mL) was added cautiously. The layers were separated, and the aqueous layer was extracted with 3 × 50 mL of diethyl ether. The combined organics were dried over $K_2CO_3$, filtered, and evaporated under reduced pressure to afford $RcCH_2OH$ as a white powder (440 mg, 1.68 mmol, 80%). $^1H$ NMR (300 MHz, benzene-$d_6$): $\delta$ 4.54 (apparent t, 2H, $J = 1.7$ Hz, $C_5H_4$), 4.37 (s, 5H, $C_5H_5$), 4.35 (apparent t, 2H, $J = 1.7$ Hz, $C_5H_4$), 4.00 (d, 2H, $J = 5.9$ Hz, $CH_2$), 1.11 (t, 1H, $J = 5.9$ Hz, OH). $^{13}C\{^1H\}$ NMR (75 MHz, benzene-$d_6$): $\delta$ 95.7 ($C_5H_4$ quat.), 70.9 ($C_5H_4$ CH), 70.6 ($C_5H_5$), 70.5 ($C_5H_4$ CH), 58.9 ($CH_2$).

**$[RcCH_2]^+[BF_4]^-$ (1a).** $HBF_4$ (ca. 2 mL of a 48% solution in diethyl ether) was added dropwise to a stirred solution of $RcCH_2OH$ (150 mg, 0.57 mmol) in diethyl ether (20 mL), resulting in an instant white precipitate. After 5 min, the

---

[57] Rybinskaya, M. I.; Kreindlin, A. Z.; Fadeeva, S. S. *J. Organomet. Chem.* **1988**, *358*, 363−374.

supernatant was removed from the precipitate by filter cannula; the precipitate was washed with diethyl ether (3 × 20 mL) and dried in vacuo. The solids were then extracted into dichloromethane (20 mL) and precipitated by dropwise addition of diethyl ether (80 mL). The supernatant was removed by filter cannula, and the solids were washed with diethyl ether (2 × 20 mL) before drying in vacuo to afford a pale cream powder (178 mg, 0.54 mmol, 92%). $^1$H NMR (300 MHz, dichloromethane-$d_2$): $\delta$ 6.26 (apparent t, 2H, $J = 1.8$ Hz, $C_5H_4$), 5.56 (s, 5H, $C_5H_5$), 5.25 (apparent t, 2H, $J = 1.8$ Hz, $C_5H_4$), 5.07 (s, 2H, $CH_2$). $^1$H NMR (300 MHz, acetone-$d_6$): $\delta$ 6.44 (m, 2H, $C_5H_4$), 5.70 (s, 5H, $C_5H_5$), 5.47 (s, 2H, $C_5H_4$), 5.25 (s, 2H, $CH_2$). $^{13}$C NMR (75 MHz, dichloromethane-$d_2$): $\delta$ 108.4 ($C_5H_4$ quat.), 93.0 ($C_5H_4$ CH), 86.7 ($C_5H_4$ CH), 84.5 ($C_5H_5$), 72.7 ($CH_2$). Anal. Calcd for $C_{11}H_{11}BF_4Ru$: C, 39.91; H, 3.35; Found: C, 39.96; H, 3.44. UV (dichloromethane): $\lambda_{max}$ 323 ($\epsilon_{323}$ 540) nm ($M^{-1}cm^{-1}$). UV (acetonitrile): $\lambda_{max}$ 319 nm. IR (KBr): 3105, 3084, 1409, 1336, 1306, 1259, 1237, 1099 (s, br), 1032 (s, br), 876, 845, 826, 806, 745, 534, 522, 502, 456, 429, 419 cm$^{-1}$. ES-MS (MeOH): *m/z* 245 (100%, $RcCH_2^+$).

**$[RcCH_2]^+[BAr'_4]^-$ (1b).** Dichloromethane (6 mL) was added to **1a** (52 mg, 0.16 mmol) and $[Na]^+[BAr'_4]^-$ [58] (127 mg, 0.14 mmol); the resulting mixture was heated under reflux for 30 min. The solvent was then removed under reduced pressure, and the remaining solids were extracted with diethyl ether (15 mL). The ether extracts were concentrated (to 3 mL) under reduced pressure, and pentane (25 mL) was added to afford a pale cream precipitate, which was washed with pentane (2 × 10 mL) and dried in vacuo (110 mg, 0.099 mmol, 69%). $^1$H NMR (300 MHz, dichloromethane-$d_2$): $\delta$ 7.72 (br s, 8H), 7.57 (s, 4H), 6.11 (apparent t, 2H, $J = 1.8$ Hz), 5.46 (s, 5H), 5.14 (apparent t, 2H, $J = 1.8$ Hz), 5.02 (s, 2H). $^{19}$F NMR (282 MHz, dichloromethane-$d_2$): $\delta$ −63.2. $^{13}$C{$^1$H} NMR (75 MHz, dichloromethane-$d_2$): $\delta$ 162.1 (q, $J_{BC} = 50$ Hz, $C_{ipso}$), 135.1 ($C_o$), 129.2 (qq, $J_{CF} = 32$, ca. 3 Hz, $C_m$), 124.9 (q, $J_{CF} = 272$ Hz, $CF_3$), 117.8 (septet, $J_{CF} =$ ca. 4 Hz, $C_p$), 108.0 ($C_5H_4$ quat.), 92.4 ($C_5H_4$ CH), 86.4 ($C_5H_4$ CH), 84.1 ($C_5H_5$), 72.1 ($CH_2$). $^{11}$B NMR (160 MHz): $\delta$ −6.25. Anal. Calcd for $C_{43}H_{23}BF_{24}Ru$: C, 46.63; H, 2.09. Found: C, 46.33; H, 2.66. IR (KBr): 3134, 1611, 1417, 1357 (s), 1278 (s), 1118 (s, br), 935, 899, 890, 841, 714, 683, 672 cm$^{-1}$.

**$[RcCH_2]^+[PF_6]^-$ (1c). Method A.** Aqueous $HPF_6$ (2 mL of a 60% solution) was added dropwise to a stirred solution of $RcCH_2OH$ (130 mg, 0.50 mmol) in THF (2 mL). After 5 min, water (40 mL) was added; the resulting creamy precipitate was washed was water (2 × 20 mL) and dried in vacuo (103 mg, 0.26 mmol, 52%). **Method B.** A solution of $[Ph_3C]^+[PF_6]^-$ (155 mg, 0.40 mmol) in dichloromethane (10 mL) was added dropwise to a stirred solution of $RcCH_2OH$ (107 mg, 0.41 mmol) in dichloromethane (10 mL). The yellow color of the trityl cation was instantly dissipated. After 5 min, the solution was filtered; diethyl ether (100 mL) was then added dropwise to precipitate a pale cream powder, which was washed with ether (2 × 20 mL) and dried in vacuo (75 mg, 0.20 mmol, 50%). $^1$H NMR (300 MHz, dichloromethane-$d_2$): $\delta$ 6.22 (apparent t, 2H, $J = 1.8$ Hz), 5.54 (s, 5H), 5.24 (apparent t, 2H, $J = 1.8$ Hz), 5.02 (s, 2H). Anal. Calcd for $C_{11}H_{11}F_6PRu$: C, 33.94; H, 2.85. Found: C, 34.25; H, 3.35. IR (KBr): 3129, 1484, 1429, 1294, 1050, 1015, 829 (s, br), 558, 492, 236, 420 cm$^{-1}$.

**$[RcCH_2]^+[CF_3SO_3]^-$ (1d).** $CF_3SO_3SiMe_3$ (ca. 0.5 mL) was added dropwise to a stirred solution of $RcCH_2OH$ (110 mg, 0.42 mmol) in diethyl ether (25 mL) at 0 °C, resulting in an instant off-white precipitate. After 20 min, the precipitate was allowed to settle; the supernatant was decanted by cannula, and the solids were washed with diethyl ether (4 × 25 mL) and dried in vacuo (130 mg, 0.33 mmol, 79%). $^1$H NMR (300 MHz, dichloromethane-$d_2$): $\delta$ 6.29 (apparent s, 2H, $C_5H_4$), 5.62 (s, 5H, $C_5H_5$), 5.29 (apparent s, 2H, $C_5H_4$), 5.09 (s, 2H, $CH_2$). $^{19}$F NMR (282 MHz, dichloromethane-$d_2$): $\delta$ −79.3. Anal. Calcd for $C_{12}H_{11}F_3O_3RuS$: C, 36.64; H, 2.82; Found: C, 36.79; H, 3.15.

**Reaction of 1,1′-Dimethylruthenocene with $[Ph_3C]^+[BF_4]^-$.** A solution of $[Ph_3C]^+[BF_4]^-$ (265 mg, 0.80 mmol) in dichloromethane (15 mL) was added dropwise to a solution of a 1,1′-dimethylruthenocene[59] (225 mg, 0.87 mmol) in dichloromethane (15 mL). The mixture slowly darkened. After 15 h the solvent was removed under reduced pressure to leave a mixture of dark oil and solid. $^1$H NMR spectroscopy revealed a complex mixture of products. Repeating the reaction at −78 °C, or using $[Ph_3C]^+[PF_6]^-$ in place of $[Ph_3C]^+[BF_4]^-$, led to no significantly different result.

**$[RcCH_2PPh_3]^+[BF_4]^-$.** $HBF_4$ (ca. 0.4 mL of a 40% aqueous solution) was added to a solution of $RcCH_2OH$ (400 mg, 1.53 mmol) and $PPh_3$ (400 mg, 1.53 mmol) in dichloromethane (2 mL). The resulting mixture was stirred for 1 h, after which diethyl ether (100 mL) was added. The white precipitate was collected on a frit, washed with diethyl ether (3 × 30 mL), and dried in vacuo at 100 °C (850 mg, 1.43 mmol, 94%). $^1$H NMR (300 MHz, chloroform-$d$): $\delta$ 7.78 (br apparent t, 3H, $J =$ ca. 7 Hz, $H_p$), 7.68−7.54 (overlapping multiplets, 12H, $H_o$ and $H_m$), 4.60 (s, 5H, $C_5H_5$), 4.39 (apparent s, 2H, $C_5H_4$), 4.29 (d, $J_{PH} = 11.5$ Hz, $CH_2$), 4.25 (apparent s, 2H, $C_5H_4$). $^{13}$C{$^1$H} NMR (75 MHz, chloroform-$d$): $\delta$ 135.1 ($C_p$), 133.9 (d, $J_{CP} = 9$ Hz, $C_o$ or $C_m$), 130.2 (d, $J_{CP} = 12$ Hz, $C_o$ or $C_m$), 117.5 (d, $J_{CP} = 85$ Hz, $C_{ipso}$), 76.1 ($C_5H_4$ quat.), 72.5 ($C_5H_4$ CH), 71.9 ($C_5H_5$), 71.0 ($C_5H_4$ CH), 26.5 (d, $J_{CP} = 45$ Hz, $CH_2$). $^{31}$P{$^1$H} NMR (122 MHz): $\delta$ 20.2. Anal. Calcd for $C_{29}H_{26}BF_4PRu$: C, 58.70; H, 4.08. Found: C, 58.15; H, 4.42. ES-MS (MeCN): *m/z* 507 (30%, $RcCH_2PPh_3^+$), 245 (100%, $RcCH_2^+$).

**Reduction of 1a with Sodium Amalgam.** A slurry of **1a** (120 mg, 0.36 mmol) in THF (30 mL) was added to an amalgam, made from 400 mg (17 mmol) of sodium and 40 g of mercury. The reaction mixture was stirred for 2 h and the organic layer decanted from the amalgam by cannula and filtered through Celite. The amalgam and Celite were washed with additional THF (3 × 20 mL), and the combined THF portions were evaporated under reduced pressure to give a white solid (90 mg). The solid was chromatographed on silica gel, initially eluting with 1:1 dichloromethane/hexane; the first fraction (ca. 1 mg, 0.004 mmol, 1%) was identified as RcMe by comparison of its $^1$H NMR spectrum with the literature.[51] A second fraction was found to be $RcCH_2CH_2Rc$ (ca. 10 mg, 0.020 mmol, 11%). $^1$H NMR (300 MHz, chloroform-$d$): $\delta$ 4.53 (s, 10H, $C_5H_4$), 4.51 (apparent t, 4H, $J = 1.6$ Hz, $C_5H_4$), 4.45 (apparent t, 4H, $J = 1.6$ Hz, $C_5H_4$), 2.35 (s, 4H, $CH_2$). $^{13}$C{$^1$H} NMR (75 MHz, chloroform-$d$): $\delta$ 92.9 ($C_5H_4$ quat.), 79.6 ($C_5H_4$ CH), 70.4 ($C_5H_5$), 69.3 ($C_5H_4$ CH), 31.2 ($CH_2$). EI-MS: *m/z* 490 (23%, $M^+$), 245 (100%, $RcCH_2^+$), 167 (15%, $RuCp^+$). A third fraction was eluted with neat dichloromethane and found to be $RcCH_2OCH_2Rc$ (ca. 18 mg, 0.035 mmol, 20%). $^1$H NMR (300 MHz, chloroform-$d$): $\delta$ 4.61 (apparent t, 4H, $J = 1.6$ Hz, $C_5H_4$), 4.49 (apparent s, 14H, $C_5H_5$ and $C_5H_4$), 4.07 (s, 4H, $CH_2$). $^1$H NMR (300 MHz, benzene-$d_6$): $\delta$ 4.66 (apparent t, 4H, $J = 1.6$ Hz, $C_5H_4$), 4.43 (s, 10H, $C_5H_5$), 4.42 (apparent t, 4H, $J = 1.6$ Hz, $C_5H_4$), 4.19 (s, 4H, $CH_2$). $^{13}$C NMR (75 MHz, chloroform-$d$): $\delta$ 87.2 ($C_5H_4$ quat.), 71.8 ($C_5H_4$ CH), 70.6 (overlapping $C_5H_4$ CH and $C_5H_5$ CH), 67.6 ($CH_2$). $^{13}$C NMR (75 MHz, benzene-$d_6$): $\delta$ 88.2 ($C_5H_4$ quat.), 72.0 ($C_5H_4$ CH), 70.9 ($C_5H_5$ CH), 70.8 ($C_5H_4$ CH), 67.8 ($CH_2$). EI-MS: *m/z* 506 (24%, $M^+$), 262 (10%, $RcCH_2O^+$ and $RcCH_2OH^+$), 245 (100%, $RcCH_2^+$), 167 (20%, $RuCp^+$).

**Crystal Structures.** Single crystals were mounted on a glass fiber using perfluoropolyether oil and cooled rapidly to 150 K in a stream of cold nitrogen using an Oxford Cryosystems CRYOSTREAM unit. Diffraction data were measured using Enraf-Nonius DIP2000 image-plate (**1b**) or Enraf-Nonius

---

[58] Brookhart, M.; Grant, B.; Volpe, A. F. *Organometallics* **1992**, *11*, 3920−3922.

[59] Lemay, G.; Kaliaguine, S.; Adnot, A.; Nahar, S.; Cozak, D.; Monnier, J. *Can. J. Chem.* **1986**, *64*, 1943−1948.

**Table 3. Summary of Crystallographic Data**

| | **1b** | **1d** | $[RcCH_2PPh_3]^+[BF_4]^- \cdot 0.5CH_2Cl_2$ |
|---|---|---|---|
| formula | $C_{43}H_{23}BF_{24}Ru$ | $C_{12}H_{11}F_3O_3RuS$ | $C_{29.5}H_{27}BClF_4PRu$ |
| fw | 1108.5 | 345.34 | 635.81 |
| cryst growth | $CH_2Cl_2$/pentane layering | $CH_2Cl_2/Et_2O$ layering | evaporation of $CH_2Cl_2$/hexane solution |
| cryst appearance | pale green prism | pale yellow fragment | colorless plate |
| cryst size/mm | 0.2 × 0.2 × 0.8 | 0.1 × 0.1 × 0.3 | 0.1 × 0.2 × 0.3 |
| space group | $C2$ | $P2_1/c$ | $C2/c$ |
| $a$/Å | 15.703(1) | 16.2555(3) | 33.0591(7) |
| $b$/Å | 12.742(1) | 13.2704(3) | 12.5182(3) |
| $c$/Å | 10.787(1) | 18.7369(5) | 13.7757(3) |
| $\beta$/deg | 97.974(4) | 104.543(2) | 101.591(1) |
| cell vol/Å$^3$ | 2137.5 | 3912.4 | 5584.7 |
| $Z$ | 2 | 12 | 8 |
| $D_c$/g mL$^{-1}$ | 1.72 | 1.76 | 1.51 |
| $\mu$/mm$^{-1}$ | 0.50 | 1.37 | 0.76 |
| $F$(000) | 1094 | 2328 | 2568 |
| max $\theta$/deg | 26.6 | 27.5 | 27.5 |
| total no. data measd | 6875 | 28 639 | 10 107 |
| total no. of unique data | 4149 | 9253 | 6308 |
| $R_{int}$ | 0.028 | 0.039 | 0.047 |
| no. of observns and criterion | 4122 ($I > 3\sigma(I)$) | 5483 ($I > 3\sigma(I)$) | 4083 ($I > 2\sigma(I)$) |
| no. params refined | 339 | 553 | 350 |
| $S$ | 1.056 | 1.025 | 1.054 |
| final $R$-indices | $R = 0.0328$ | $R = 0.0371$ | $R1 = 0.0632$ ($I > 2\sigma(I)$) |
| | $R_w = 0.0398$ | $R_w = 0.0494$ | $wR2 = 0.1607$ ($I > 2\sigma(I)$) |
| min and max residuals/e Å$^{-3}$ | −0.70, 1.48 | −0.76, 1.23 | −1.069, 1.689 |

Kappa CCD diffractometers (**1d** and $[RcCH_2PPh_3]^+[BF_4]^- \cdot 0.5CH_2Cl_2$), in each case with graphite-monochromated Mo Kα radiation, $\lambda = 0.71069$ Å. Intensity data were processed using the programs DENZO and SCALEPACK.[60] Structures were solved by direct methods using SIR92,[61] which located all non-hydrogen atoms. Subsequent full-matrix least-squares refinement was carried out against observed $F$ using the CRYSTALS program suite[62] (for **1b** and **1d**) or against all $F^2$ using SHELXS-97[63] within WinGX[64] (for $[RcCH_2PPh_3]^+[BF_4] \cdot 0.5CH_2Cl_2$). Coordinates and anisotropic thermal parameters of all non-hydrogen atoms were refined. Further details of the crystal structure determinations are given in Table 3 and in the Supporting Information.

For **1b**, both the Ru and B atoms lie on a crystallographic 2-fold rotation axis. The tetraarylborate anion is positioned on the axis such that the crystallographic symmetry coincides with the local symmetry of the molecule. However, the symmetry requires the cation to be disordered. The cation has been modeled as positioned with the Ru atom lying directly on the axis with the cyclopentadienyl and fulvene ligands disordered in such a way that their five-membered rings overlap. The acceptable geometry and thermal ellipsoids shown in Figure 2 indicate that this is a good approximation. The large thermal parameters of some of the peripheral F atoms of the anion suggest that the $CF_3$ groups may be disordered, but attempts to model this did not result in any improvement of the fit to the data.

The unit cell of **1d** contains three crystallographically distinct triflate anions, which have no crystallographic symmetry, and four distinct $\mathbf{1}^+$ cations. Two of these—those containing Ru(3) and Ru(4)—lie on crystallographic centers of inversion, with the five-membered cyclopentadienyl and fulvene rings of each cation superimposed by the crystallographic disorder. One of the other cations—that containing Ru(2)—has no crystallographic symmetry, but also appears to be disordered as some C atoms have large anisotropic thermal parameters and there is significant residual electron density nearby; this disorder could not be successfully modeled. The remaining cation (that containing Ru(1)) appears to be completely ordered, as do all three crystallographically distinct triflate anions; these four moieties also have no crystallographic symmetry.

The asymmetric unit of $[RcCH_2PPh_3]^+[BF_4]^- \cdot xCH_2Cl_2$ contains one cation and one anion, with no crystallographic symmetry, and a dichloromethane molecule which was modeled with one Cl atom on a 2-fold rotation axis, with the rest of the molecule disordered as a result of the crystallographic symmetry. There is therefore half (or less) of a dichloromethane molecule in the asymmetric unit. $^1H$ NMR spectroscopy of some of the crystals dissolved in $CDCl_3$ confirmed that $x =$ ca. 0.5. The thermal parameters of the tetrafluoroborate ion are suggestive of some disorder around a noncrystallographic 3-fold axis, and one of the phenyl rings also appears slightly disordered. Attempts to model the disorder in these groups did not lead to any improvement in the refinement.

**Computational Methods.** Calculations were performed using the density functional methods of the Amsterdam Density Functional Package (ADF 2000.2).[65-67] Type IV basis sets were used with triple-ζ accuracy sets of Slater-type orbitals, with a single polarization function added to the main group atoms. The cores of the atoms were frozen up to 2p for Fe, 3p for Ru, and 1s for C. First-order relativistic corrections were made to the cores of the atoms. Relativistic corrections were included using the ZORA formalism. Three different

---

(60) Otwinowski, Z., Minor, W., Carter, C. W., Sweet, R. M., Eds.; *DENZO* and *SCALEPACK*; Academic Press: New York, 1997; Vol. 276.

(61) Altomare, A.; Cascarano, G.; Giacovazzo, C.; Guagliardi, A.; Polidori, G.; Burla, M. C.; Camalli, M. *J. Appl. Crystallogr.* **1994**, *27*, 435.

(62) Watkin, D. J.; Prout, C. K.; Carruthers, J. R.; Betteridge, P. W.; *CRYSTALS issue 10*; Chemical Crystallography Laboratory: Oxford, UK, 1996.

(63) Sheldrick, G. M. *SHELXS 97, Program for Crystallography*; University of Göttingen: Göttingen, Germany, 1997.

(64) Ferrugia, L. J. *WinGX: An Integrated System of Publically Available Windows Programs for the Solution, Refinement, and Analysis of Single-Crystal X-ray Diffraction Data*; University of Glasgow: Glasgow, UK, 1998.

(65) te Velde, G.; Baerends, E. J. *J. Comput Phys.* **1992**, *99*, 84−98.

(66) Baerends, E. J.; Berces, A.; Bo, C.; Boerringter, P. M.; Cavallo, L.; Deng, L.; Dickson, R. M.; Ellis, D. E.; Fan, L.; Fischer, T. H.; Fonseca Guerra, C.; van Gisbergen, S. J.; Groeneveld, J. A.; Gritsenko, O. V.; Harris, F. E.; van den Hoek, P.; Jacobsen, H.; van Kessel, G.; Kootstra, F.; van Lenthe, E.; Osinga, V. P.; Philipsen, P. H. T.; Post, D.; Pye, C. C.; Ravenek, W.; Ros, P.; Schipper, P. R. T.; Schreckenbach, G.; Snijiders, J. G.; Sola, M.; Swerhone, D.; te Velde, G.; Vernooijis, P.; Versluis, L.; Visser, O.; van Wezenbeek, E.; Wiesenekker, G.; Wolff, S. K.; Woo, T. K.; Ziegler, T. *ADF Program System Release 1999*; Department of Theoretical Chemistry, Vrije Universiteit: Amsterdam, 1999.

(67) Guerra, C. F.; Snijders, J. G.; te Velde, G.; Baerends, E. J. *Theor. Chem. Acc.* **1998**, *99*, 391−403.

procedures were used for optimization. The local density approximation of Vosko, Wilk, and Nusair[68] was used throughout. First, no gradient correction was used. Second, the nonlocal exchange corrections by Becke[69] and nonlocal correlation corrections by Perdew were used.[70] Third, Becke exchange[69] and Lee, Wang, and Parr correlation[71] corrections were made (BLYP method).

**Acknowledgment.** The authors thank Johnson-Matthey PLC for a generous loan of $RuCl_3 \cdot xH_2O$, the EPSRC for a studentship (T.J.B.), Juan Manríquez for drawing our attention to his metathesis method of obtaining $[BAr'_4]^-$ salts, a referee for drawing our attention to ref 56, and Colin Sparrow for acquiring electrospray mass spectra.

**Supporting Information Available:** Tables of crystal structure solution and refinement details, atomic coordinates and equivalent isotropic displacement parameters, bond lengths and angles, anisotropic displacement parameters, hydrogen coordinates, and isotropic displacement parameters for **1b**, **1d**, and $[RcCH_2PPh_3]^+[BF_4]^- \cdot 0.5CH_2Cl_2$. This material is available free of charge via the Internet at http://pubs.acs.org.

OM010667+

---

(68) Vosko, S. H.; Wilk, L.; Nusair, M. *Can. J. Phys.* **1990**, *58*, 1200.
(69) Becke, A. D. *Phys. Rev.* **1988**, *A38*, 3098−3100.
(70) Perdew, J. P. *Phys. Rev.* **1986**, *B34*, 8822−8824.
(71) Lee, C. T.; Yang, W. T.; Parr, R. G. *Phys. Rev.* **1988**, *B37*, 785−789.